HIGH-RESOLUTION IMAGERY DATA TO ASSESS THE SPATIAL VARIABILITY OF SUGARCANE FIELDS/ DADOS DE IMAGENS DE ALTA RESOLUÇÃO PARA AVALIAÇÃO DA VARIABILIDADE ESPACIAL DE TALHÕES DE ….

Article *in* Brazilian Journal of Development · January 2020

DOI: 10.34117/bjdv6n12-500

CITATIONS
0

READS
26

5 authors, including:

Tatiana Fernanda Canata
University of São Paulo
23 PUBLICATIONS **42** CITATIONS
SEE PROFILE

Leonardo Felipe Maldaner
University of São Paulo
28 PUBLICATIONS **51** CITATIONS
SEE PROFILE

Jose Paulo Molin
University of São Paulo
249 PUBLICATIONS **1,726** CITATIONS
SEE PROFILE

High-resolution imagery data to assess the spatial variability of sugarcane fields

Dados de imagens de alta resolução para avaliação da variabilidade espacial de talhões de cana-de-açúcar

DOI:10.34117/bjdv6n12-500

Recebimento dos originais:08/11/2020
Aceitação para publicação:20/12/2020

João Pedro Pissolito
Discente em Engenharia Agronômica
Instituição: Universidade de São Paulo, Escola Superior de Agricultura "Luiz de Queiroz", ESALQ/USP, Departamento de Engenharia de Biossistemas
Endereço: Av. Pádua Dias, 11, Piracicaba – SP, Brasil
E-mail: jppissolito@usp.br

Victor Hugo Sousa Bersani
Engenheiro Agrônomo
Instituição: Pedra Agroindustrial S/A
Endereço: Av. Caramuru, 1280, Ribeirão Preto – SP, Brasil
E-mail: victor.bersani@usp.br

Tatiana Fernanda Canata
Mestra em Ciências
Instituição: Universidade de São Paulo, Escola Superior de Agricultura "Luiz de Queiroz", ESALQ/USP, Departamento de Engenharia de Biossistemas
Endereço: Av. Pádua Dias, 11, Piracicaba – SP, Brasil
E-mail: tatiana.canata@usp.br

Leonardo Felipe Maldaner
Mestre em Ciências
Instituição: Universidade de São Paulo, Escola Superior de Agricultura "Luiz de Queiroz", ESALQ/USP, Departamento de Engenharia de Biossistemas
Endereço: Av. Pádua Dias, 11, Piracicaba – SP, Brasil
E-mail: leonardofm@usp.br

José Paulo Molin
Professor PhD
Instituição: Universidade de São Paulo, Escola Superior de Agricultura "Luiz de Queiroz", ESALQ/USP, Departamento de Engenharia de Biossistemas
Endereço: Av. Pádua Dias, 11, Piracicaba – SP, Brasil
E-mail: jpmolin@usp.br

ABSTRACT
The vegetation index (VI) generated from orbital images are essential tools to identify the spatial variability of the crops. The objective of this study was to evaluate the spatial variability of sugarcane fields using imagery data. Also, to explore the ideal period to correlate the Normalized Difference Vegetation Index (NDVI), Normalized Difference Red-Edge Index (NDRE) and Wide Dynamic Range Vegetation Index (WDRVI) with sugarcane yield. Four fields were selected in the state of São Paulo (56.37 ha) during the 2017/2018 and 2018/2019 growing seasons, as well as five fields in the state of Goiás (86.86 ha) during the 2019/2020 growing season. The VIs were calculated using orbital images from Sentinel-2 (spatial resolution of 10 m). The yield data were generated by a commercial sensor-system installed on the harvesters with a resolution of 0.20 Hz. Yield data were filtered and interpolated using the same resolution of the orbital images. Pearson's correlation was calculated between the yield and the VIs for each orbital image. The considered VIs were able to identify the spatial variability of sugarcane fields with coefficients of correlation of 0.95 and 0.96. The sugarcane stalks growth was the best period to correlate the VIs and the yield maps among the analyzed fields.

Keywords: precision agriculture, remote sensing, vegetation indexes, yield.

RESUMO
Os índices de vegetação (IV) gerados a partir de imagens orbitais são ferramentas essenciais para identificar a variabilidade espacial das culturas. O objetivo deste estudo foi avaliar a variabilidade espacial de lavouras de cana-de-açúcar por meio de imagens orbitais. Assim como, explorar o período ideal para correlacionar *Normalized Difference Vegetation Index* (NDVI), *Normalized Difference Red-Edge Index* (NDRE) e *Wide Dynamic Range Vegetation Index* (WDRVI) com a produtividade da cana-de-açúcar. Foram selecionados quatro talhões no estado de São Paulo (56,37 ha) durante as safras 2017/2018 e 2018/2019, bem como cinco talhões no estado de Goiás (86,86 ha) durante a safra 2019/2020. Os IVs foram calculados utilizando imagens orbitais do Sentinel-2 (resolução espacial de 10 m). Os dados de produtividade foram gerados por meio de sensores comerciais instalados nas colhedoras com resolução de 0,20 Hz. Os dados de produtividade foram filtrados e interpolados com a mesma resolução das imagens orbitais. A correlação de Pearson foi calculada entre a produtividade e os IVs para cada imagem orbital. Os IVs avaliados foram capazes de identificar a variabilidade espacial dos canaviais com coeficientes de correlação de 0,95 e 0,96. O período de crescimento dos colmos da cana-de-açúcar foi considerado como sendo o melhor para correlacionar os IVs com os mapas de produtividade nos talhões analisados.

Palavras-Chave: agricultura de precisão, sensoriamento remoto, índices de vegetação, produtividade.

1 INTRODUCTION

Brazil is the world's major producer of sugarcane followed by India and China (FAO, 2018). The first production forecast of 2020/2021 season is about 642.07 million tons of sugarcane (*Saccharum officinarum* L.) with an average yield of 76.35 t ha^{-1} (CONAB, 2020). The sugarcane development cycle is divided in sprouting, tillering, stalk growth and maturation stages. The first phase, sprouting, lasts about 30 days after cutting (DAC); the tillering occurs since 30 up to 120 DAC; the

stalk growth starts at 120 DAC and can achieve until 270 DAC; the last phase before harvester, maturation, occurs between 270 and 360 DAC (DIOLA and SANTOS, 2010).

The sugarcane vegetative growth is irregular over the production fields (AMARAL et al., 2015a). This is variability enables the use of precision agriculture (PA) practices, based on monitoring the spatial and temporal variability looking for management strategies to maximize profitability and minimize negative environmental impacts with the rational use of agricultural inputs (MOLIN et al., 2015). However, the sugarcane producers yet do not use yield maps (AMARAL et al., 2015b), which is the most important data in crop management, as it is the response of the crop to the management carried out. Traditionally, a low data density has been used for the decision-making process, not useful for PA applications, which needs a dense and spatialized data. Bramley (2009) states that the identification of the spatial variability of fields and the measurement of agricultural production can be performed by indirect methods, such as remote sensing (RS) techniques.

The correct use of orbital images can improve the traditional methods of crop monitoring and together with other data sources; it can be used to predict crop yields (RAHMAN and ROBSON, 2016; DALLA MARTA et al., 2013; LIAQAT et al., 2017; NAGY et al., 2018). The acquisition of orbital images during the production phase and over the production years, allows the temporal evaluation of the biomass variability of agricultural crops (MOREL et al., 2014). Kayad et al. (2018) used Sentinel-2 images and machine learning techniques to assess corn yield variability at field scale. Moreover, temporal RS data, combined with yield and soil characteristics, can be used to identify different management zones (MZ) within the fields (MULLA, 2013).

Fernandes et al. (2017) showed that VIs calculated from orbital images could infer about sugarcane yield. NDVI has been one of the most common VI to estimate plants biomass; however, this VI is susceptible to the saturation effect, which intensifies with the increase in the leaf area index and with large biomass production, like sugarcane (RAHMAN and ROBSON, 2016). Amaral et al. (2015b) found that NDRE is less susceptible to saturation effect than NDVI because it normally reaches the maximum value at a more advanced sugarcane stage. The NDVI is a benchmark for the development of new VIs (HATFIELD et al., 2008) with specific changes in the weight of some spectral bands, such as the WDRVI (SAKAMOTO et al., 2011; SAKAMOTO et al., 2013). However, there are limited studies in the literature relating sugarcane canopy reflectance, and high-resolution spatial yield data (ABDEL-RAHMAN and AHMED, 2008). The objective of this study was to explore the best period, within the development cycle of sugarcane, to correlate the VIs generated from high-resolution imagery data with yield data.

2 MATERIAL AND METHODS

Four fields (56.37 ha) were selected in São Manuel, São Paulo, Brazil. The climate is classified as Cfa according to the Köppen's climate classification (ALVARES et al., 2013). Also, five fields (86.86 ha) were selected in Chapadão do Céu, Goiás, Brazil. According to Alvares et al. (2013) the climate is classified as Am. Both commercial areas were mechanically harvested, and the row spacing adopted was 1.50 m. The 2017/2018 (São Manuel, São Paulo), 2018/2019 (São Manuel, São Paulo), and 2019/2020 (Chapadão do Céu, Goiás) growing seasons were named as scenarios A, B, and C, respectively. Table 1 describes the characteristics of the selected sugarcane fields.

Table 1. Study scenarios and characteristics of the selected sugarcane fields

Scenario	Field	Area (ha)	Variety	Ratoon	Harvest date[1]	Geographical coordinates
A	F1 F2 F3 F4	13.97 11.70 12.65 18.05	SP-832847	4th	10/14/2017	22° 41’ 25.48” S; 48° 16’ 42.89” W
B	F1 F2 F3 F4	13.97 11.70 12.65 18.05	SP-832847	5th	11/11/2018	22° 41’ 25.48” S; 48° 16’ 42.89” W
C	F1 F2 F3 F4 F5	10.77 5.26 22.02 18.26 30.55	RB-55156	4th	05/31/2019	18° 01’ 37.96” S; 52° 39’ 10.94” W

[1]Date of reference considered to calculate the days after cutting for each orbital image

The spatiotemporal analyses of the VIs were performed considering the 12-month cycle of the crop, identifying each period by the DAC, according to the classification of Diola and Santos (2010). The Sentinel-2 data was downloaded from EarthExplorer website (https://earthexplorer.usgs.gov/) selecting low cloud cover (<1%) of the areas of interest. There were used 30, 33 and 15 orbital images in scenarios A, B, and C, respectively. Each field was delimited by a polygon, removing data from borders of internal roads (internal buffer of 5.0 m). Table 2 describes the spectral bands used in the study and the respective resolutions. The radiometric correction of the images was performed with the free Semi-Automatic Classification plugin (CONGEDO, 2016) in QGIS 3.4 (Open Source Geospatial Foundation, Beaverton, USA) which provides tools for atmospheric/radiometric correction to the original orbital images.

Table 2. Spectral bands resolution of Sentinel-2

Spectral Bands	Central wavelength (nm)	Resolution		
		Spatial (m)	Temporal (days)	Radiometric (bits)
B4 - Red	665	10	5	12
B8 - NIR	842			
B5 - Red-edge	705	20		

Red = reflectance in the red region; Red-edge = reflectance in the transition region between red and near infrared; NIR = reflectance in the near infrared region

The NDVI (ROUSE et al., 1974), NDRE (BARNES et al., 2000), and WDRVI (GITELSON, 2004) were calculated according to equations 1, 2 and 3, respectively, for all orbital images.

$$NDVI = \frac{NIR - Red}{NIR + Red} \quad (1)$$

$$NDRE = \frac{NIR - Red\text{-}edge}{NIR + Red\text{-}edge} \quad (2)$$

$$WDRVI = \frac{\propto . NIR - Red}{\propto . NIR + Red} \quad (3)$$

where: Red = reflectance in the red region (~ 665 nm); Red-edge = reflectance in the transition region between red and near infrared (~ 705 nm); NIR = reflectance in the near infrared region (~ 842 nm).

Gitelson (2004) recommended the weighting coefficient (a) between 0.10 and 0.20 for WDRVI calculation. Maresma et al. (2016) stated that the most appropriate weighting coefficient to estimate the nitrogen dose and corn yield was 0.10. Therefore, the value of 0.10 was assumed for the weighting coefficient of WDRVI.

The yield data was generated by a commercial sensor-system (Solinftec, Araçatuba, São Paulo, Brazil) installed on the harvesters. The data was georeferenced by a GNSS- RTK (Real Time Kinematic) receiver. The frequency of data acquisition was 0.20 Hz, and the travel speed of the harvester was about 1.25 m s^{-1}. The original yield data were filtered to eliminate the outliers using the methodology described by Maldaner and Molin (2020), and the interpolation was performed using Vesper 1.6 software (MINASNY et al., 2006) considering the kriging method, which considers the spatial dependence between the points. The semivariogram model adopted was that with the lowest Root Mean Square Error (RMSE). The spatial resolution of the generated yield maps was 10 m, the same spatial resolution of the orbital images. The pixel by pixel correlation between the yield and VIs maps was calculated using Pearson's correlation coefficient (r) using the software RStudio (Integrated Development for R, Boston, USA).

3 RESULTS AND DISCUSSION

The descriptive statistics of the yield maps for scenarios A, B and C are shown in Table 3. The average yield of the scenario A was 64.04 t ha^{-1}, and in scenario B was 70.47 t ha^{-1}. For the scenario C was 94.95 t ha^{-1}. The difference between the average yield of the scenarios A and B was 6.43 t ha^{-1} (the same production environment). The yield difference between the scenarios A and C was 30.91 t ha^{-1}, and between the scenarios B and C was 24.48 t ha^{-1}. Thus, it is noted that scenario C had higher average values of yield than scenarios A and B.

Table 3. Descriptive statistics of sugarcane yield data for each field from different scenarios

		Yield (t ha^{-1})				
Scenarios		**Field 1**	**Field 2**	**Field 3**	**Field 4**	**Field 5**
A	n	1,369	1,138	1,245	1,779	-
	Mean	63.99	64.26	65.07	62.84	-
	Median	65.24	64.54	64.82	63.00	-
	Minimum	42.74	50.02	46.28	49.19	-
	Maximum	79.46	76.51	81.97	75.21	-
	SD	6.61	4.95	6.68	4.56	-
	CV (%)	10.33	7.71	10.26	7.26	-
B	N	1,399	1,165	1,267	1,807	-
	Mean	72.28	75.76	71.69	62.14	-
	Median	71.57	76.61	74.30	62.96	-
	Minimum	10.28	0	15.89	0	-
	Maximum	95.27	110.65	102.02	93.31	-
	SD	7.54	14.21	14.19	9.57	-
	CV (%)	10.43	18.76	19.79	15.41	-
C	n	1,074	526	2,203	1,827	3,056
	Mean	95.16	95.62	95.66	97.49	90.81
	Median	95.63	95.66	96.94	98.40	91.58
	Minimum	87.04	89.79	81.90	86.17	79.17
	Maximum	99.80	99.53	105.22	105.64	105.04
	SD	2.66	1.50	4.59	4.58	4.90
	CV (%)	2.80	1.57	4.80	4.69	5.39

n: number of samples; SD: standard deviation; CV: coefficient of variation

The coefficient of variation (CV) is an indicative of variability. The yield data variability was low, according to Pimentel-Gomes and Garcia (2002) criteria, in Fields 2 and 4, and moderate for Fields 1 and 3 in the scenario A; moderate in all fields of scenario B and low in all fields of scenario C, where also the difference between the average yield was relatively low, varying between 90.81 t ha^{-1} and 97.49 t ha^{-1}.

The semivariogram model for yield data was the exponential in scenario A, with the lowest RMSE (0.83 t ha^{-1}), and in scenario B with an RMSE of 6.44 t ha^{-1}. For the scenario C, the spherical model showed the lowest RMSE (0.19 t ha^{-1}). The geostatistical analysis showed the yield was spatially

more dependent in scenarios A and C than in B, due to the lower variation of the nugget effect (KARP, 2018). Table 4 shows the semivariogram parameters obtained for yield data from three study scenarios.

Table 4. Semivariogram parameters for interpolation of sugarcane yield data

Scenarios	Model	Nugget	RMSE (t ha^{-1})	Sill	Range (m)
A	Exponential	10.48	0.83	53.00	55.57
B	Exponential	540.60	6.44	929.20	19.31
C	Spherical	26.04	0.19	50.59	233.40

RMSE: root mean square error

Figures 1, 2 and 3 show the average values of NDVI, NDRE and WDRVI as a function of DAC of the analyzed fields, as well the coefficients of correlation between the VIs and the sugarcane yield data for scenarios A, B and C, respectively.

Figure 1. Average values of the VIs and coefficients of correlation for field 1 (a); field 2 (b); field 3 (c); field 4 (d) in the study scenario A

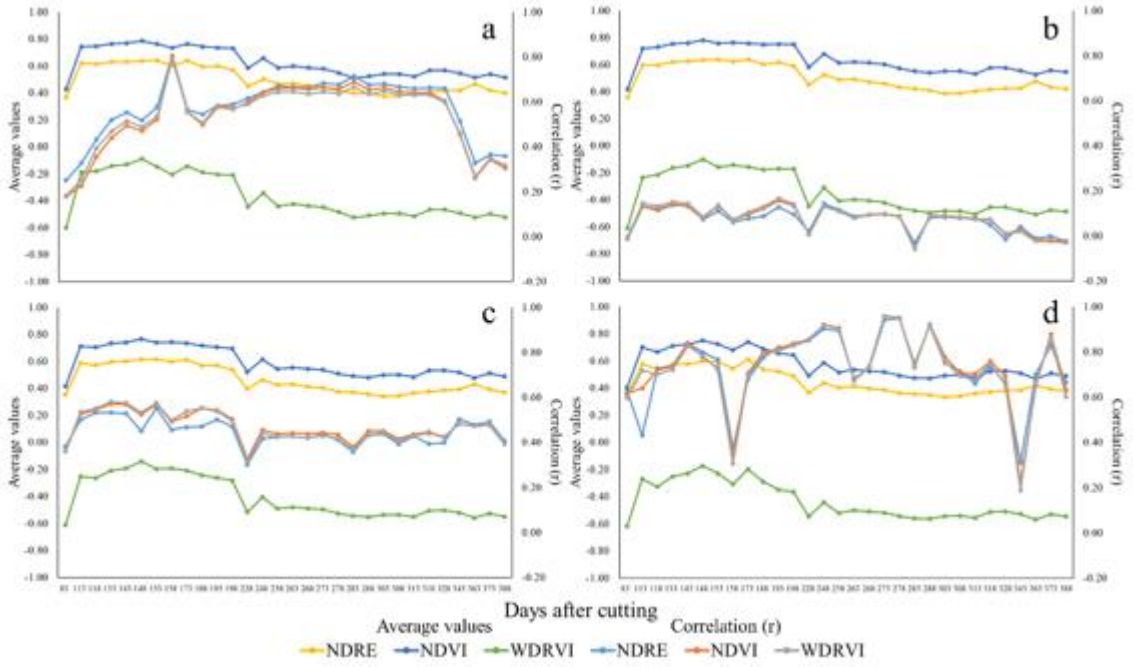

Figure 2. Average values of the VIs and coefficients of correlation for field 1 (a); field 2 (b); field 3 (c); field 4 (d) in the study scenario B

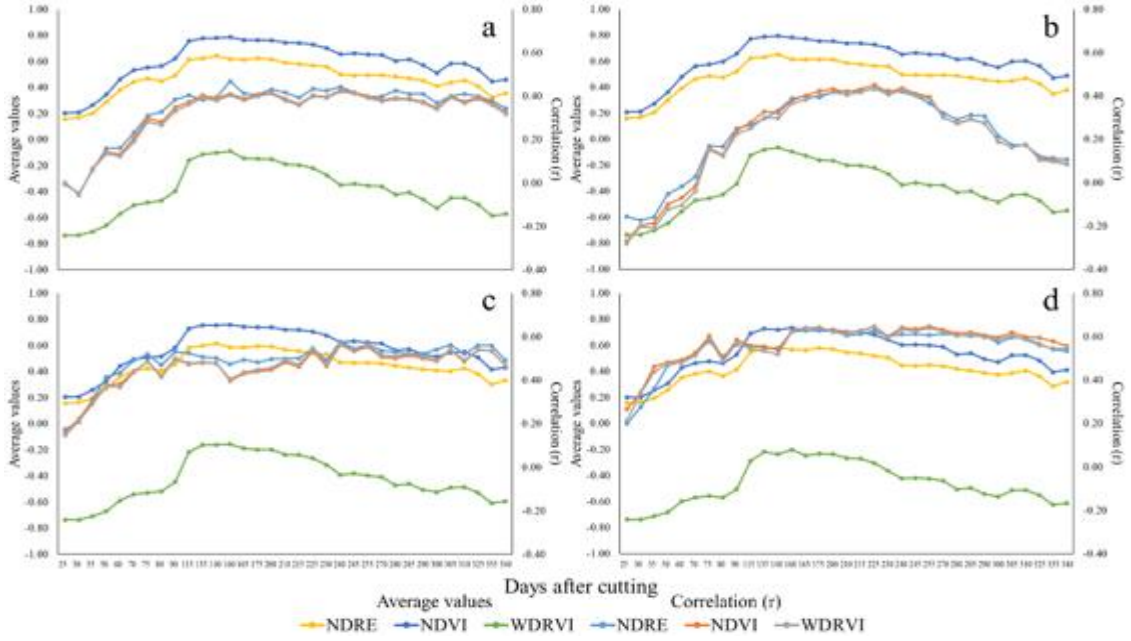

Figure 3. Average values of the VIs and coefficients of correlation for field 1 (a); field 2 (b); field 3 (c); field 4 (d); field 5 (e) in the study scenario C

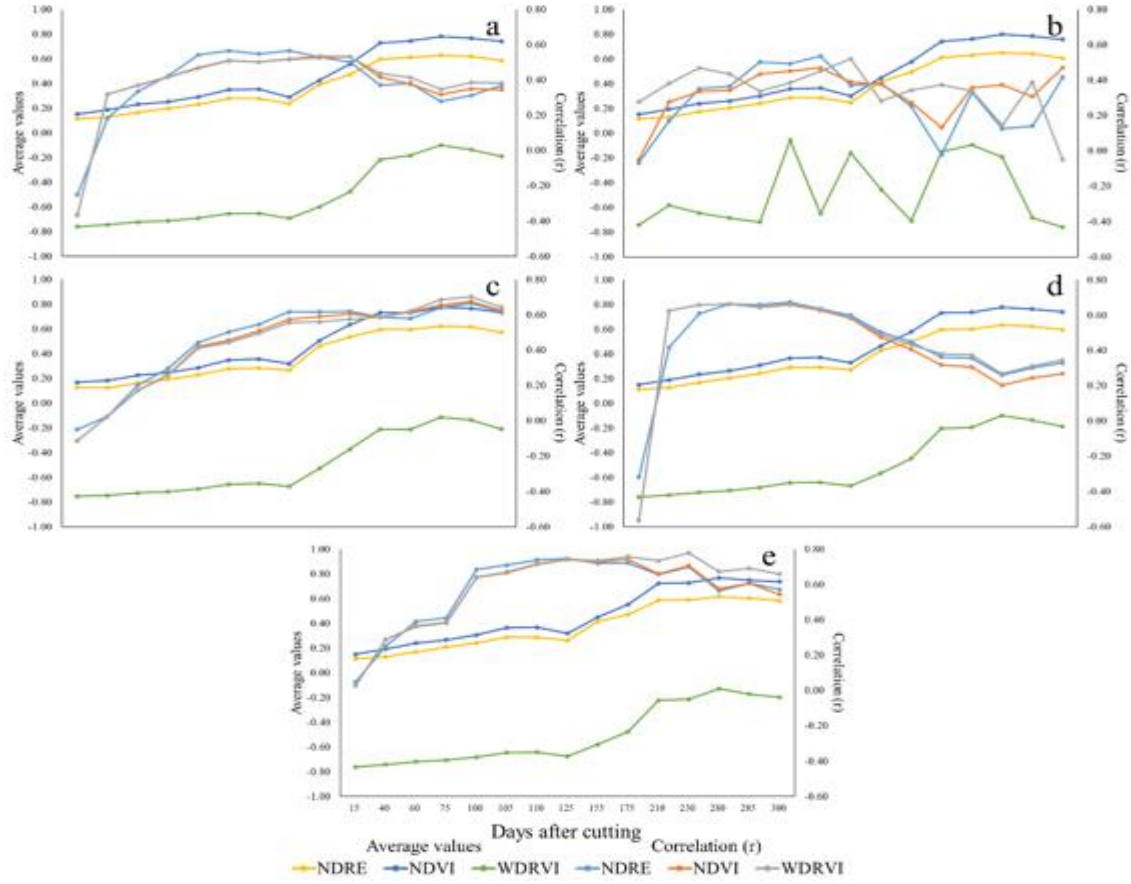

High correlation values between the VIs and the sugarcane yield during the sugarcane stalks growth, and at the beginning of maturation stage, were observed. For scenario C, in addition to the stalk growth stage and in the initial stage of maturation, there was a high correlation during the tillering crop stage. Therefore, the sugarcane stalks growth was the best correlation period found, since it was repeated in the three scenarios among the results.

NDVI shows greater reflectance values than NDRE. According to Lucas and Schuler (2007) the highest average values of NDVI occur during the sugarcane vegetative period, from 120 to 270 DAC. A decrease for average values of the VI during the maturation stage, from 270 DAC, was observed. The VI showed the best correlations with yield predominantly in the period of growth of sugarcane stalks in all the study scenarios and fields. Amaral et al. (2015b) obtained reasonable correlation (r = 0.81) for both NDVI and NDRE from canopy sensors and biomass when the sugarcane stalk height was 0.5 m. Rocha et al. (2019) identified that NDRE associated with the number and height of the sugarcane stalks, can assist in the prediction of biomass in the early stages of the crop.

Sugarcane yield maps; NDVI at 133, 158, 193 and 273 DAC (Fields 3, 1, 2 and 4 respectively); NDRE at 153, 158, 248 and 278 DAC (Fields 3, 1, 2 and 4 respectively); and WDRVI at 133, 158, 193 and 273 DAC (Fields 3, 1, 2 and 4 respectively) in the study scenario A are shown in Figure 4 (variables with the highest correlation with sugarcane yield data).

Figure 4. Sugarcane yield maps (a); the VIs maps as a function of DAC in the study scenario A for NDVI (b); NDRE (c); WDRVI (d)

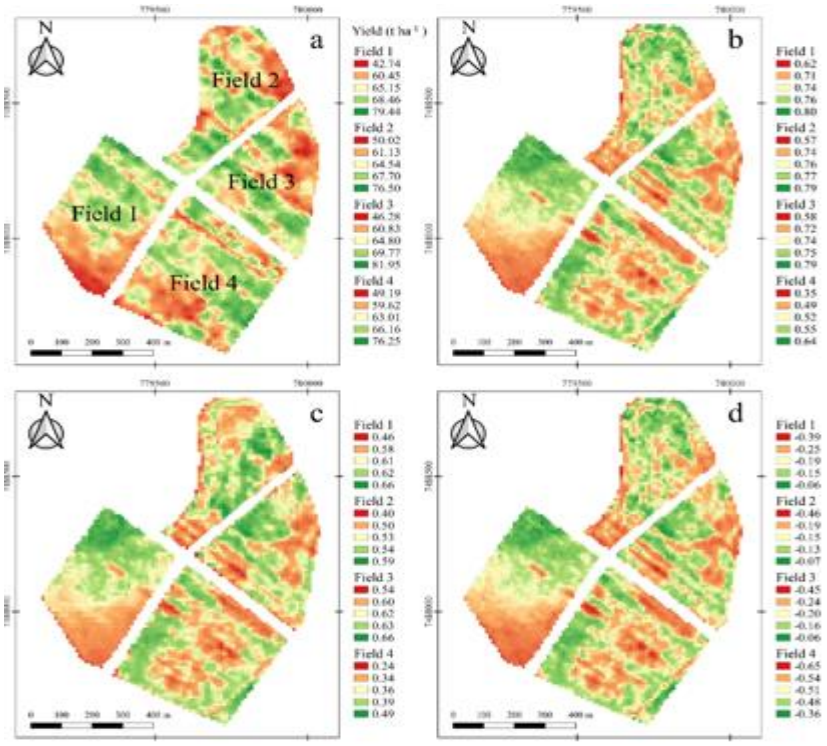

Sugarcane yield maps; NDVI at 225, 225, 240 and 240 DAC (Fields 2, 4, 1 and 3 respectively); NDRE at 160, 165, 225 and 240 DAC (Fields 1, 4, 2 and 3 respectively); and WDRVI at 175, 225, 240 and 240 DAC (Fields 4, 2, 1 and 3 respectively) in the study scenario B are shown in Figure 5 (variables with the highest correlation).

Figure 5. Sugarcane yield maps (a); The VIs maps as a function of DAC in the study scenario B for NDVI (b); NDRE (c); WDRVI (d)

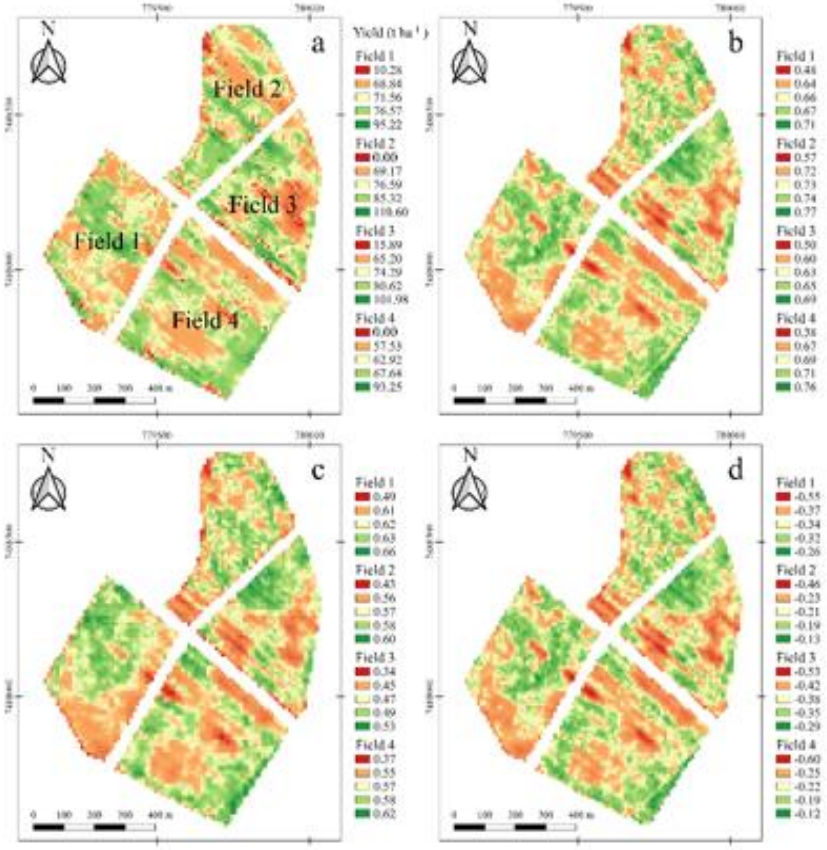

Sugarcane yield maps; NDVI at 75, 125, 155, 285 and 300 DAC (Fields 4, 5, 1, 3 and 2 respectively); NDRE at 105, 110, 125, 125 and 285 DAC (Fields 4, 2, 1, 5 and 3 respectively); and WDRVI at 105, 125, 175, 230 and 285 DAC (Fields 4, 2, 1, 5 and 3 respectively) in the study scenario C are shown in Figure 6 (variables with the highest correlation).

Figure 6. Sugarcane yield maps (a); The VIs maps as a function of DAC in the study scenario C for NDVI (b); NDRE (c); WDRVI (d)

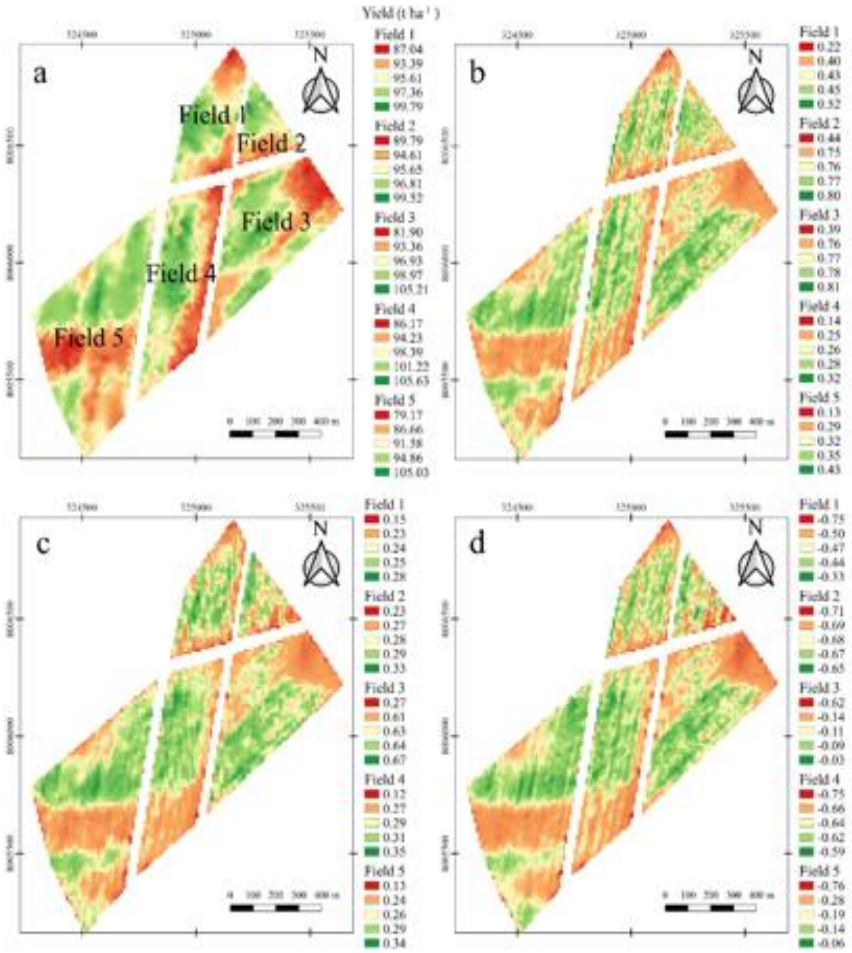

The VIs had potential to identify the spatial variability of sugarcane fields, since the yield was acquired using data in high-resolution (about 200 final points ha-1). One of the reasons is the time slot between the last reasonable reflectance data from canopy and harvest, normally under dry conditions, what makes it challenging to predict yield with good accuracy, but it has already been useful to identify spatial variability of the sugarcane fields.

From the VIs maps it is possible to identify the spatial variability inherent to the fields, demonstrating that the sugarcane yield and the crop vigor were not uniform. The presence of locals with higher or lower yield can be caused by different agronomic factors (soil, weather, etc.), which need further investigation. Spatial variability can be explored by developing management strategies at low resolution, such as considering the range values of yield, with regions of the field separated into MZ, or by a pixel resolution, with different amounts of inputs and other treatments (ADAMCHUK et al., 2004). The VIs also can be useful to outline MZ because they identify different spectral behaviors of the crop development over the season (ZHANG et al., 2010; CHANG et al., 2014).

The results of this study indicate that the real yield data is necessary to relate it with RS information and more investigation is necessary to identify the potential of high-resolution images for estimating sugarcane yield. In parallel, agronomic investigations are requirement to identify factors that cause spatial variability of crop yield to support in decision-making process for optimizing sugarcane production.

4 CONCLUSION

The spatial variability of sugarcane fields was verified qualitatively from the VIs generated based on orbital images from Sentinel-2. The level of the spatial variability on sugarcane fields was determined considering the sugarcane yield and the VIs maps for different scenarios. The best period to correlate sugarcane yield and VIs was during the sugarcane growth stalks stage. NDVI was that demonstrated the highest spatial correlation values.

ACKNOWLEDGEMENTS

The authors gratefully acknowledge the operational support provided by Solinftec, São Manoel, and CerradinhoBio sugar mills. To the National Council for Scientific and Technological Development (Conselho Nacional de Desenvolvimento Científico e Tecnológico – CNPq) for the scientific initiation scholarship granted to J.P.P. and V.H.S.B. and for granting a graduate scholarship to L.F.M (Grant No. 168643/2017-0). To the Coordination for the Improvement of Higher Education Personnel (Coordenação de Aperfeiçoamento de Pessoal de Nível Superior – CAPES – Finance Code 001) for the graduate scholarship provided to T.F.C. Also, to the Luiz de Queiroz Agrarian Studies Foundation (Fundação de Estudos Agrários Luiz de Queiroz – FEALQ) by the financial support of the article publication.

REFERENCES

Abdel-Rahman, E. M., and Ahmed, F. B (2008) The application of remote sensing techniques to sugarcane (Saccharum spp. hybrid) production: a review of the literature. International Journal of Remote Sensing. 29, p. 3753-3767.

Adamchuk, V. I., Hummel, J. W., Morgan, M. T., and Upadhyaya, S. K. (2004) On-the-go soil sensors for precision agriculture. Computers and Electronics in Agriculture. 44, p. 71-91.

Alvares, C. A., Stape, J. L., Sentelhas, P. C., Gonçalves, J. L. M., and Sparovek, G. (2013) Köppen's climate classification map for Brazil. Meteorologische Zeitschrift. 22, p. 711-728.

Amaral, L. R., Molin, J. P., and Schepers, J. S. (2015a) Algorithm for variable-rate nitrogen application in sugarcane based on active crop canopy sensor. Agronomy Journal. 107, p. 1513-1523.

Amaral, L. R., Molin, J. P., Portz, G., Finazzi, F. B., and Cortinove, L. (2015b) Comparison of crop canopy reflectance sensors used to identify sugarcane biomass and nitrogen status. Precision Agriculture. 16, p. 15-28.

Barnes, E. M., Clarke, T. R., Richards, S. E., Colaizzi, P. D., Haberland, J., Kostrzewski, M., Waller, P., Choi, C., Riley, E., Thompson, T., Lascano, R. J., Li, H., and Moran, M. S. (2000) Coincident detection of crop water stress, nitrogen status and canopy density using ground-based multispectral data. Proceedings of the Fifth International Conference on Precision Agriculture, Bloomington, MN, USA. July 16th -19th, pp. 1-15.

Bramley, R. G. V. (2009) Lessons from nearly 20 years of Precision Agriculture research, development, and adoption as a guide to its appropriate application. Crop and Pasture Science. 60, p. 197-217.

Chang, D., Zhang, J., Zhu, L., Ge, S. H., Li, P. Y., and Liu, G. S. (2014) Delineation of management zones using an active canopy sensor for a tobacco field. Computers and Electronics in Agriculture. 109, p. 172-178.

CONAB. Companhia Nacional de Abastecimento (2020) Acompanhamento da safra brasileira de cana-de-açúcar. Available online at https://www.conab.gov.br/info-agro/safras/cana. Accessed in: August 21th, 2020 (in Portuguese).

Congedo, L. (2016) Semi-automatic classification plugin - Usermanual. Technical Report.
Dalla Marta, A., Grifoni, D., Mancini, M., Orlando, F., Guasconi, F., and Orlandini, S. (2013) Durum wheat in-field monitoring and early-yield prediction: assessment of potential use of high resolution satellite imagery in a hilly area of Tuscany, Central Italy. Journal of Agricultural Science. 153, p. 68-77.

Diola, V.; and Santos, F. Fisiologia. In: Santos, F.; Borém, A.; and Caldas, C. (2010) Cana-de-açúcar: bioenergia, açúcar e álcool: tecnologias e perspectivas, Editora UFV, Viçosa, MG, Brazil (in Portuguese).

FAO. Food and Agriculture Organization of the United Nations (2018) FAO no Brasil. Available online at http://www.fao.org/tc/cplpunccd/paginas-nacionais/brasil/en/. Accessed in: October 7th, 2019.

Fernandes, J. L., Ebecken, N. F. F., and Esquerdo, J. C. D. M. (2017) Sugarcane yield prediction in Brazil using NDVI time series and neural networks ensemble. International Journal of Remote Sensing. 38, p. 4631-4644.

Gitelson, A. A. (2004) Wide dynamic range vegetation index for remote quantification of biophysical characteristics of vegetation. Journal Plant Physiology. 161, p. 165-173.

Hatfield, J. L., Gitelson, A. A., Schepers, J. S., and Walthall, C. L. (2008) Application of spectral remote sensing for agronomic decisions. Agronomy Journal. 100, p. 117-131.

Karp, F. H. S. (2018) Spatial variability of canopy geometric parameters in a commercial coffee field. Final Paper. College of Agriculture "Luiz de Queiroz", University of São Paulo, Piracicaba, SP, Brazil.
Kayad, A., Sozzi, M., Gatto, S., Marinello, F., and Pirotti, F. (2019) Monitoring within-field variability of corn yield using Sentinel-2 and machine learning techniques. Remote Sensing. 11, 2873.

Liaqat, M. U., Cheema, M. J. M., Huang, W., Mahmood, T., Zaman, M., and Khan, M. M. (2017) Evaluation of MODIS and Landsat multiband vegetation indices used for wheat yield estimation in irrigated Indus Basin. Computers and Electronics in Agriculture. 138, p. 39-47.

Lucas, A. A., and Schuler, C. A. B. (2007) Análise do NDVI/NOAA em cana-de-açúcar e Mata Atlântica no litoral norte de Pernambuco. Revista Brasileira de Engenharia Agrícola e Ambiental. 11, p. 607-614 (in Portuguese).

Maldaner, L. F.; and Molin, J. P. (2020) Data processing within rows for sugarcane yield mapping. Scientia Agricola. Available online at https://www.scielo.br/scielo.php?script=sci_arttext&pid=S0103-90162020000500101. Accessed in: August 21th, 2020.

Maresma, Á., Ariza, M., Martínez, E., Lloveras, J., and Martínez-Casasnovas, J. A. (2016) Analysis of vegetation Indices to determine nitrogen application and yield prediction in maize (Zea mays L.) from a standard UAV service. Remote Sensing. 8, p. 973.

Minasny, B., McBratney, A. B., and Walvoort, D. J. J. (2007). The variance quadtree algorithm: use for spatial sampling design. Computers and Geosciences. 33, p. 383-392.

Molin, J. P., Colaço, A. F., and Amaral, L. R. (2015) Agricultura de Precisão, Oficina de Textos, Piracicaba, SP, Brazil (in Portuguese).

Morel, J., Todoroff, P., Bégué, A., Bury, A., Martiné, J. F., and Petit, M. (2014) Toward a satellite-based system of sugarcane yield estimation and forecasting in smallholder farming conditions: a case study on Reunion Island. Remote Sensing. 6, p. 6620-6635.

Mulla, D. J. (2013) Twenty five years of remote sensing in precision agriculture: key advances and remaining knowledge gaps. Biosystems Enginering. 114, p. 358-371.

Nagy, A., Fehér, J., and Tamas, J. (2018) Wheat and maize yield forecasting for the Tisza river catchment using MODIS NDVI time series and reported crop statistics. Computers and Electronics in Agriculture, 151, p. 41-49.

Pimentel-Gomes, F., and Garcia, C. H. (2002) Estatística aplicada a experimentos agronômicos e florestais, Fealq, Piracicaba, SP, Brazil (in Portuguese).

Rahman, M. M., and Robson, A. J. (2016) A Novel Approach for sugarcane yield prediction using Landsat time series imagery: a case study on Bundaberg region. Advances in Remote Sensing. 5, p. 93-102.

Rocha, M. G., Barros, F. M. M., Oliveira, S. R. M., and Amaral, L. R. (2019) Biometric characteristics and canopy reflectance association for early-stage sugarcane biomass prediction. Scientia Agricola. 76, p. 274-280.

Rouse, J. W., Haas, R. H., Schell, J. A., and Deering, D. W. (1974) Monitoring vegetation systems in the great plains with ERTS. Proceedings of the Third Earth Resources Technology Satellite Symposium, Washington, DC, USA. pp. 309-317.

Sakamoto, T., Gitelson, A. A., and Arkebauer, T. J. (2013) MODIS-based corn grain yield estimation model incorporating crop phenology information. Remote Sensing of Environment. 131, p. 215-231.

Sakamoto, T., Gitelson, A. A., Wardlow, B. D., Verma, S. B., and Suyker, A. E. (2011) Estimating daily gross primary production of maize based only on MODIS WDRVI and shortwave radiation data. Remote Sensing of Environment. 115, p. 3091-3101.

Zhang, X., Shi, L., Jia, X., Seielstad, G., and Helgason, C. (2010) Zone mapping application for precision-farming: a decision support tool for variable rate application. Precision Agriculture.11, p. 103-114.